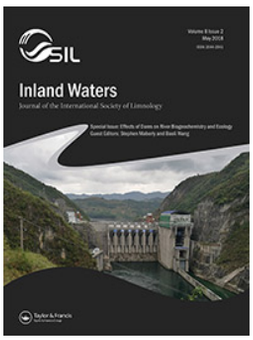

Inland Waters

ISSN: 2044-2041 (Print) 2044-205X (Online) Journal homepage: http://www.tandfonline.com/loi/tinw20

Spatial variation of nitrogen cycling in a subtropical stratified impoundment in southwest China, elucidated by nitrous oxide isotopomer and nitrate isotopes

Fu-Jun Yue, Si-Liang Li, Cong-Qiang Liu, Khan M.G. Mostofa, Naohiro Yoshida, Sakae Toyoda, Shi-Lu Wang, Shohei Hattori & Xiao-Long Liu

To cite this article: Fu-Jun Yue, Si-Liang Li, Cong-Qiang Liu, Khan M.G. Mostofa, Naohiro Yoshida, Sakae Toyoda, Shi-Lu Wang, Shohei Hattori & Xiao-Long Liu (2018) Spatial variation of nitrogen cycling in a subtropical stratified impoundment in southwest China, elucidated by nitrous oxide isotopomer and nitrate isotopes, Inland Waters, 8:2, 186-195, DOI: 10.1080/20442041.2018.1457847

To link to this article: https://doi.org/10.1080/20442041.2018.1457847

Published online: 14 Jun 2018.

INLAND WATERS
2018, VOL. 8, NO. 2, 186–195
https://doi.org/10.1080/20442041.2018.1457847

Spatial variation of nitrogen cycling in a subtropical stratified impoundment in southwest China, elucidated by nitrous oxide isotopomer and nitrate isotopes

Fu-Jun Yue [a,b] Si-Liang Li,[c,d] Cong-Qiang Liu,[a] Khan M.G. Mostofa [d] Naohiro Yoshida [e] Sakae Toyoda,[e] Shi-Lu Wang [a] Shohei Hattori,[e] and Xiao-Long Liu[f]

[a]State Key Laboratory of Environmental Geochemistry, Institute of Geochemistry, Chinese Academy of Sciences, Guiyang, China; [b]School of Geographical and Earth Sciences, University of Glasgow, Glasgow, UK; [c]State Key laboratory of Hydraulic Engineering Simulation and Safety, Tianjin University, Tianjin, China; [d]Institute of Surface-Earth System Science, Tianjin University, Tianjin, China; [e]Department of Environmental Science and Technology, Tokyo Institute of Technology, Yokohama, Japan; [f]Tianjin Key Laboratory of Water Resources and Environment, Tianjin Normal University, Tianjin, China

ABSTRACT

Estimates of biogeochemical processes and the proportion of N_2O production in the aquatic system of impoundments are important to quantify nitrogen cycling, particularly during stratification periods. In this study, we used the dual isotopes of nitrate (NO_3^-) and nitrous oxide (N_2O) to estimate the nitrogen dynamics and contributions to N_2O production and reduction at varying zones in Lake Baihua, located in southwest China. The lake was strongly stratified during the sampling period, with the oxic zone from the surface to 12 m and the anoxic zone from 12 to 21 m. The assimilation shifted $\delta^{15}N$ and $\delta^{18}O$ of NO_3^- significantly in the epilimnion (0–4 m), and denitrification contributed to the shift in the low dissolved oxygen zone of the hypolimnion. The semiquantitative analysis showed that nitrification accounted for >67% of the N_2O production between 0 and 4 m while higher nitrification contributions were also found between 6 and 12 m. The contribution of denitrification between 15 and 21 m was >43%. The mechanism responsible for the vertical variations should be considered in the estimation of nitrogen cycling and N_2O production in subtropical stratified impoundments.

ARTICLE HISTORY
Received 18 July 2017
Accepted 1 February 2018

KEYWORDS
denitrification; N_2O isotopomer; nitrate isotopes; nitrification; stratified lake

Introduction

Lakes are considered a large global sink for reactive nitrogen (Pearson et al. 2012, Finlay et al. 2013). Nitrogen (N) dynamics in lake ecosystems involve a series of complex processes, such as external inputs and internal biogeochemical cycles; however, the effects of freshwater N removal are still poorly understood (Mayer and Wassenaar 2012, Finlay et al. 2013, Wenk et al. 2014). In general, nitrate (NO_3^-) is the dominant form of dissolved inorganic nitrogen (DIN) entering aquatic environments. Globally, concentrations of NO_3^- are steadily increasing in aquatic systems, which has been attributed to increasing surface run-off, river damming, aquaculture, N deposition, agricultural, and other land-based activities (Sterner 2011, Mostofa et al. 2013, North et al. 2013, Beusen et al. 2016). High levels of NO_3^- in freshwaters are detrimental to human and ecosystem health and sustainability (Ohte et al. 2010, Finlay et al. 2013, Beusen et al. 2016).

Lakes are most likely to become important N sinks under stratified conditions, especially for anoxic bottom water. Conditions in the surficial bottom sediments of lakes that favor denitrification processes are due to high organic matter inputs from the overlying water column and strong dissolved oxygen (DO) gradients. Denitrification processes in stratified lakes primarily occur in the redox transition zone, which is largely controlled by the oxygen supply via hydrodynamic processes and the consumption of oxidants due to organic matter degradation (Pearson et al. 2012, Wenk et al. 2014). Nitrous oxide (N_2O) can be produced by the N cycle as a by-product of hydroxylamine (NH_2OH) oxidation during nitrification processes as well as during incomplete denitrification processes (Sasaki et al. 2011, Wenk et al. 2016) and can contribute to global warming and stratospheric ozone depletion (Well et al. 2005).

Stable isotope analysis, particularly the dual isotope approach of NO_3^- and N_2O, is a powerful tool that can provide critical insights into N transformation dynamics in lakes (Spoelstra et al. 2001, Xiao and Liu 2004, Finlay et al. 2007, Ohte et al. 2010, Sasaki et al. 2011, Mayer and Wassenaar 2012, Wenk et al. 2014, 2016). For example, the values of dual NO_3^- isotopes would increase during biological processes in aquatic environments, such as

CONTACT Si-Liang Li siliang.li@tju.edu.cn

uptake by algae or denitrification by bacteria. Previous studies showed that the $\delta^{15}N$ and $\delta^{18}O$ isotopic ratio was maintained at 1:1 during assimilation (Granger et al. 2010, Mayer and Wassenaar 2012) but increased to ~2:1 during denitrification (Mayer and Wassenaar 2012, Wenk et al. 2014).

The ^{15}N-site preference (SP), namely the difference in isotopic ^{15}N between the central (α) and terminal (β) positions within the asymmetric N_2O molecule, can be defined as $SP = \delta^{15}N^{\alpha} - \delta^{15}N^{\beta}$ (Toyoda and Yoshida 1999). The characteristic isotopic signature of N_2O can be used to determine different sources of N_2O and its microbial pathways (Yoshida et al. 1989, Toyoda et al. 2005, Sutka et al. 2006, Yamagishi et al. 2007, Wenk et al. 2016). Previous studies have used SP as a diagnostic tool to elucidate source processes of N_2O, such as nitrification and denitrification (Sutka et al. 2003, Baggs 2008, Frame and Casciotti 2010, Santoro et al. 2011, Heil et al. 2014). For example, the SP signature of N_2O via nitrite (NO_2^-) or NO_3^- reduction, whether by nitrifying or denitrifying bacteria, can be as low as −10.7‰, clearly lower than that from N_2O produced by nitrification (e.g., ammonia and hydroxylamine oxidation, up to 37.5‰; Sutka et al. 2006, Frame and Casciotti 2010). In addition, fungal denitrification yields N_2O with an SP value of 37‰, which is close to nitrification but considerably different from that produced during bacterial denitrification (Sutka et al. 2008). Finally, pure culture studies provide compelling evidence suggesting that SP values of 0‰ or less are indicative of N_2O produced by denitrifying bacteria while SP values of 30.6‰–7.5‰ indicate N_2O produced from hydroxylamine oxidation or fungal denitrification (Sutka et al. 2006, Frame and Casciotti 2010, Wu et al. 2016).

Hydroelectric impoundments are widely distributed in southwest (SW) China. High levels of N_2O and its emission to the atmosphere have been found from those reservoirs (Liu et al. 2011). Constructed in 1966, Lake Baihua (BH) is a typical hydroelectric impoundment in SW China with a series of 8 dams along the Maotiao River, located in the upper reaches of Wujiang, a tributary of the Changjiang (Yangtze) River of China. BH is a eutrophic lake with a high content of dissolved organic matter (up to 330 μM C) and high primary production with chlorophyll concentration up to 66 μg/L (Fu et al. 2010). Previous studies showed that the production and consumption of N_2O in BH strongly accord with the decomposition of organic matter during lake stratification, and the emission flux of N_2O is high (2.4 $\mu molm^2/h$; Wang et al. 2004, Liu 2010). However, the proportion of N_2O production from various processes is not well constrained in hydroelectric impoundments of SW China. Relatively high concentrations of NO_3^- and N_2O along with high contents of dissolved organic matter in BH make it ideal for studying N processes in subtropical impoundments, which can provide vital information for understanding processes for many lakes with similar conditions around the globe. To understand the processes leading to the production of N_2O, however, it is imperative to explore the N cycle in the whole water column. As such, the goal of this study was to assess NO_3^- and N_2O transformation in this subtropical lake during summer stratification periods. We report new measurements to estimate the concentration and isotopic composition of NO_3^- and N_2O in the water column to assess their spatial variation as well as to identify their fate. The major transformations of nitrification and denitrification contributed to N_2O production and reduction in different water depths were also estimated based on SP values.

Study site

BH is located near Guiyang, SW China, at an altitude of ~1200 m a.s.l. The mean annual precipitation in the area is ~1200 mm. The valleys upstream and downstream of BH are both long and narrow, but the middle section of the lake is wide, with >100 islands distributed in the lake (Fig. 1). Another hydroelectric impoundment, Lake Hongfeng (HF) built in 1960, is situated upstream of BH. The water discharged from HF (30.2 m^3/s) is the primary water source for BH (38 m^3/s; Liu 2010). These 2 impoundments serve to control floods and provide water for electrical power generation, industrial and

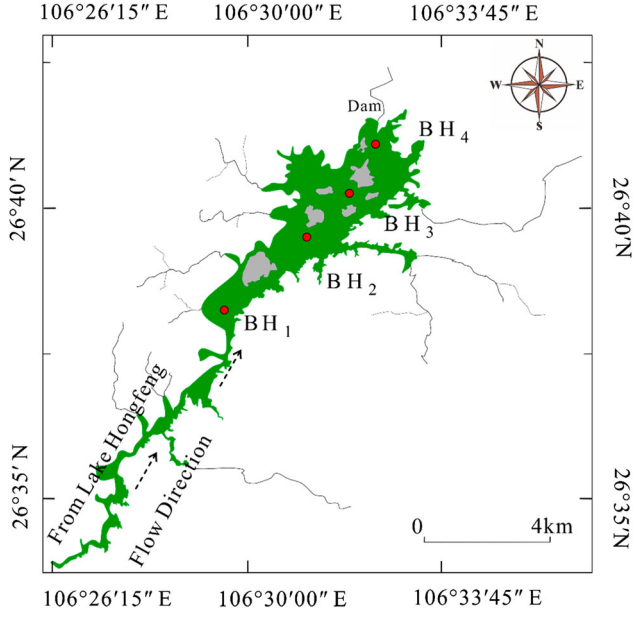

Figure 1. Lake Baihua sampling sites, denoted by circles. The gray areas within the lake represent islands.

agricultural water supply, and recreation. The water level fluctuates between 1240 m (normal level) and 1227.5 m (storage level) a.s.l. in HF, and between 1195 m and 1188 m a.s.l. in BH, influenced by engineered water control and climate (Liu 2010). Stratification can be observed frequently between April and August in BH (Wang et al. 2004).

Methods

Water sampling was conducted in BH during August 2013. To understand the spatial variations in N cycles within the entire lake system, 4 sampling sites were chosen along the lake (Fig. 1). Specifically, the first sampling site (BH_1) was located at the upper reach, the second (BH_2) was near one of the tributaries located in the middle section, the third (BH_3) was located in the lower reach, and the fourth (BH_4) was located ~0.5 km upstream of the dam. Water flow was from BH_1 to BH_4 (Fig. 1). Profiles of temperature (T), DO, and conductivity (EC) were obtained with an automated multiparameter monitoring instrument (Yellow Springs Instruments: YSI 6600 v2). A 5-L Niskin water sampler was used to collect water samples at the same depths at which T, DO, and EC were measured. Water samples were filtered through 0.45 μm membrane filters (Millipore) and kept at 4 °C in the dark until analysis. Concentrations of ammonium (NH_4^+), NO_2^-, NO_3^-, and total dissolved nitrogen for the filtered samples were analyzed using an automatic flow analyzer (SKALAR Sans Plus Systems) within 48 h. The concentrations of dissolved organic carbon (DOC) were analyzed as CO_2 by the wet oxidation method (Aurora 1030). Water samples were first acidified with 5% (vol/vol) of H_3PO_4 to remove all inorganic carbon, and then 10% $Na_2S_2O_8$ was added to oxidize organic carbon to inorganic carbon.

The NO_3^- isotopes of water samples were measured by the denitrifer method (McIlvin and Casciotti 2011). Four international NO_3^- (USGS-32, USGS-34, USGS-35, and IAEA-N3) and 2 experimental reference materials were used for the calibration. The precision for the samples analyzed in duplicates was 0.3‰ for $\delta^{15}N$ and 0.5‰ for $\delta^{18}O$ of NO_3^-.

Water samples for N_2O isotopomer analysis were directly sampled into 120 mL glass bottles sealed with butyl rubber stoppers. The samples were injected with 0.6 mL of $HgCl_2$ solution (5%) and stored at 4 °C until analysis. Bulk N_2O isotope and isotopomer analyses were conducted at the Tokyo Institute of Technology, Japan, using an online analytical system with a stainless steel gas transfer line, pre-concentration traps, chemical traps for removal of H_2O and CO_2, and a gas chromatograph/isotope ratio mass spectrometer (MAT 252; Thermo Fisher Scientific Inc.; Toyoda and Yoshida 2016). The detailed description of the calibrated method and process for measuring N_2O concentrations and isotopomer can be found in Toyoda and Yoshida (2016). The $\delta^{15}N$ and $\delta^{18}O$ were reported relative to atmospheric N_2 and V-SMOW, respectively.

Results

Because of the shallow depth at BH_1, the depth profiles of T, DO, and DOC (Fig. 2) were limited to 10 m. The T profiles in the epilimnion zone were similar at all 4 sites (Fig. 2a); however, below the thermocline (~6–10 m), the depth-profiles of T remained similar between the 2 middle sites (i.e., BH_2 and BH_3) but were notably different at the other 2 sites. The mixing discharge at site BH_4, with a constant T value between 15 and 21 m, may be caused by continuous water flow at the suboxic hypolimnion zone toward the dam. The DO values ranged from 223 to 338 μmol/L (μM) from the surface to the depth of 4 m and then decreased rapidly between the depth of 4 and 8 m (Fig. 2b). Low DO (<20 μM) was detected at 10 m at BH_1 and below 12 m at the other 3 sites. Thus, the oxic zone extended from the surface to about 12 m, and the anoxic zone was roughly from 12 m to the lake bottom. In addition, DO values between the surface and 6 m were higher at the upper section of the lake (i.e., BH_1) and gradually decreased toward the lower reaches (i.e., BH_4). This decreasing trend in DO along the water flow direction was probably caused by O_2 degassing and consumption of oxygen by degradation of organic matter. As the major recharge source of BH, the water discharged from HF with low T (13.7 °C) can increase dissolution of O_2 into the water, but the increased temperature of water during the water flow may lead to O_2 degassing. Although DOC concentrations were relatively constant

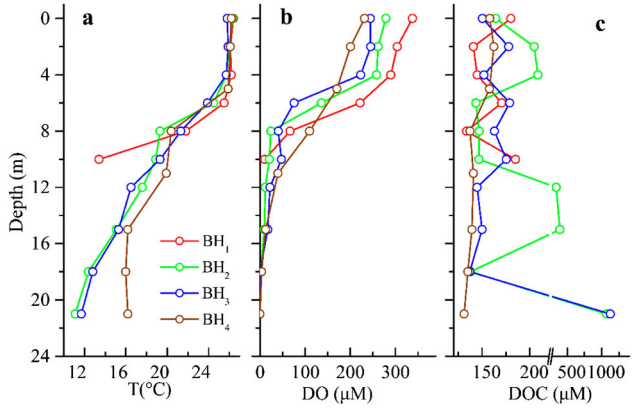

Figure 2. Water column profiles of (a) temperature, (b) DO, and (c) dissoved organic carbon in Lake Baihua during August 2013.

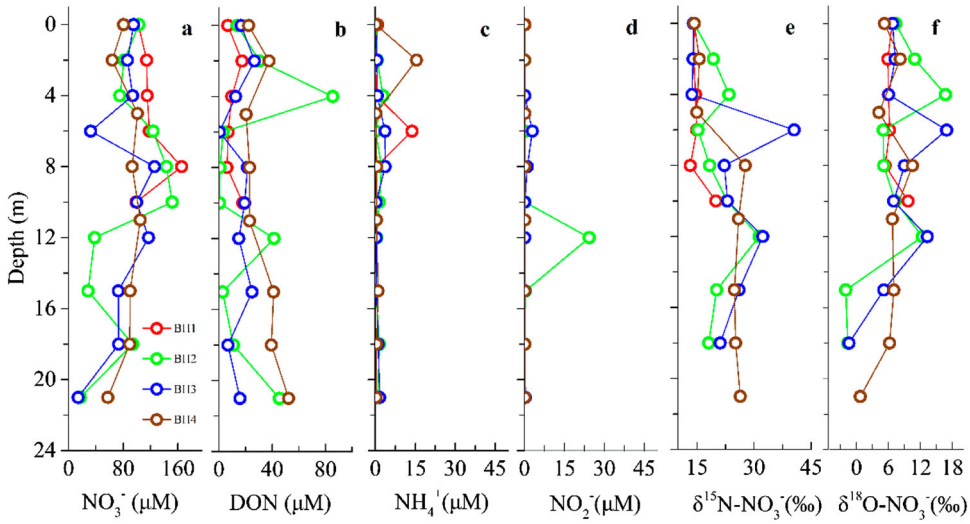

Figure 3. Water column profiles of (a) dissolved NO_3^-, (b) DON, (c) NH_4^+, (d) NO_2^-, (e) $\delta^{15}N-NO_3^-$, and (f) $\delta^{18}O-NO_3^-$ in Lake Baihua during August 2013.

at BH_4, they varied greatly with depth at BH_2 and BH_3, where higher DOC concentrations were found at deeper depths (Fig. 2c).

The depth profiles of NO_3^-, dissolved organic nitrogen (DON), NH_4^+, NO_2^-, and dual NO_3^- isotopes at the 4 sampling sites (Fig. 3) show that the average concentration of NO_3^- over the depth profile was highest at BH_1 (mean [1 SD] = 119 [24] μM) and decreased in the lower reaches with (86 [47] μM) at BH_2, (81 [35] μM) at BH_3, and (85 [17] μM) at BH_4 (Fig. 3a). NO_3^- concentrations were relatively constant above 4 m, but in the deeper water its concentrations fluctuated greatly with depth and among sites (Fig. 3a).

The average concentration of DON over the depth profile was lower at BH_1 (10.8 [5.5] μM) and increased monotonically from BH_2 (15.9 [8.0] μM) to BH_3 (23.4 [27.6] μM) and BH_4 (33.3 [12.3] μM; Fig. 3b). DON at BH_2 showed the greatest fluctuation with depth among all sampling sites, with higher values at 4, 12, and 21 m. Significant negative relationships between DON and NO_3^- existed at all sites except for BH_2, which were indicative of the contribution of NO_3^- from degradation of organic N (Fig. 4a).

NH_4^+ and NO_2^- were minor forms of DIN while NO_3^- and DON were the dominant forms of dissolved N (Fig. 3c). The concentrations of NH_4^+ and NO_2^- were low (<4 μM) for most depth profiles. The NH_4^+ concentration was highest at 6 m at BH_1 and 2 m at BH_4 (Fig. 3c), and NO_2^- concentration was highest at 12 m at BH_2 (Fig. 3d).

The isotopic composition of NO_3^- varied markedly with depth at all 4 sites (Fig. 3e). The average $\delta^{15}N$ of NO_3^- over the depth profile increased from 15.2‰ (2.4‰) at BH_1 to 20.3‰ (5.1‰) at BH_2 and 23.0‰ (9.1‰) at BH_3 and then decreased slightly to 21.8‰ (5.8‰) at BH_4. The average $\delta^{18}O$ of NO_3^- over the

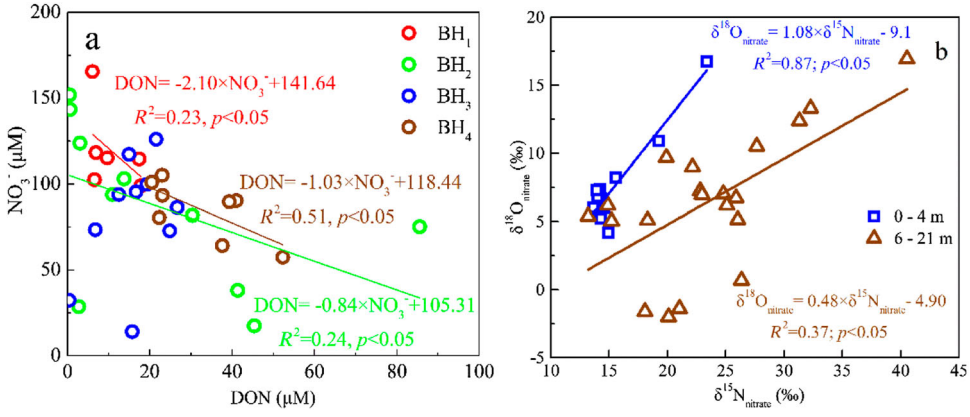

Figure 4. The relationship between (a) NO_3^- and DON and between (b) $\delta^{15}N-NO_3^-$ and $\delta^{18}O-NO_3^-$ in Lake Baihua during the summer stratified period.

depth profile varied from 6.7‰ (1.6‰) at BH_1 to 6.8‰ (6.1‰) at BH_2, 7.8‰ (5.1‰) at BH_3, and 6.1‰ (2.9‰) at BH_4. The NO_3^- isotope peaks occurred at the top of the anoxic zone (between 4 and 6 m). However, $\delta^{18}O$ of NO_3^- tended to decrease with depth, and negative values were measured at 15 and 18 m at BH_2 and BH_3, respectively. Increasing $\delta^{15}N$ and $\delta^{18}O$ of NO_3^- with decreasing NO_3^- concentrations were also observed in a few water samples taken from the epilimnion and in most of the water samples taken from the hypoxic hypolimnion. The highest $\delta^{15}N$ value was 40.5‰ at 6 m at BH_3 and the highest $\delta^{18}O$ value was also observed at the same depth at BH_3 with a value of 16.9‰. In addition, the $\delta^{15}N$ and $\delta^{18}O$ values of NO_3^- were relatively stable from 0 to 8 m at BH_1 and below 12 m at BH_4, whereas those values fluctuated at BH_2 and BH_3, closely resembling the trends in NO_3^- and DON concentration profiles. A 1:1 slope line existed between $\delta^{18}O$ of NO_3^- and $\delta^{15}N$ of NO_3^- for the water samples taken from the depths between 0 and 4 m (Fig. 4b).

The N_2O concentrations varied substantially among the sampling sites ranging from 15 to 850 nmol/L (nM), and the average values increased from 33.9 (27.4) nM at BH_1, to 77.1 (81.4) nM at BH_2, to 213 (274) nM at BH_3 and then decreased to 45.4 (27.5) nM at BH_4 (Fig. 5a). Extreme oversaturation levels (e.g., 1.6–71-fold) of N_2O with respect to atmospheric equilibrium were detected at different depths. Three water profiles had N_2O peaks at 8 m, associated with the rapid decrease in DO concentrations (Fig. 5a and 2b). Although the N_2O peak at BH_4 occurred at 11 m, it occurred at analogous DO concentrations to other depth profiles with high concentrations of N_2O (Fig. 5a and 2b) and was associated with the lowest bulk $\delta^{15}N$ (−8.3‰). The highest N_2O concentration was detected at the bottom of BH_3, which also had the highest DOC concentration. The stable isotopic composition of N_2O at BH_1 was relatively constant with depth, except that a peak value occurred at 8 m, which corresponded to the depth of the peak concentration of N_2O (Fig. 5a–b).

The bulk $\delta^{15}N$ of N_2O ranged from −8.3‰ to 26.9‰ for the 4 water depth profiles. The average values of bulk $\delta^{15}N$ were 2.8‰ (1.8‰) at BH_1, 6.8‰ (8.7‰) at BH_2, 2.0‰ (2.9‰) at BH_3, and 2.8‰ (9.2‰) at BH_4. The bulk $\delta^{18}O$ values of N_2O ranged from 16.1‰ to 55.1‰ among the 4 depth profiles, and their average values were 26.7‰ (5.3‰) at BH_1, 36.8‰ (6.8‰) at BH_2, 31.8‰ (6.0‰) at BH_3, and 32.9‰ (14.2‰) at BH_4. The bulk $\delta^{15}N$ and $\delta^{18}O$ were higher at 12 m and then decreased to the bottom at BH_2; however, the bulk $\delta^{15}N$ decreased from 8 m to the bottom and $\delta^{18}O$ decreased from 12 m to the bottom at BH_3.

The average SP values of N_2O were higher in the upper (29.2‰ [11.1‰] at BH_1) and lower (33.0‰ [16.8‰] at BH_4) reaches compared to the 2 middle sites (26.9‰ [9.0‰] at BH_2 and 20.4‰ [9.7‰] at BH_3). The SP values were higher at 8 and 15 m and subsequently decreased to the bottom for 3 profiles.

Discussion

Nitrate transformation and cycling along with its isotopic characteristics in Lake Baihua

Compared to other sites, BH_1 showed higher NO_3^- concentrations and lower NO_3^- isotopes at almost all depths, indicating different NO_3^- sources or different processes. Degradation of organic N (e.g., organic N → NH_4^+ → NO_3^-; mineralization and nitrification), which is primarily released from phytoplankton by both photochemical

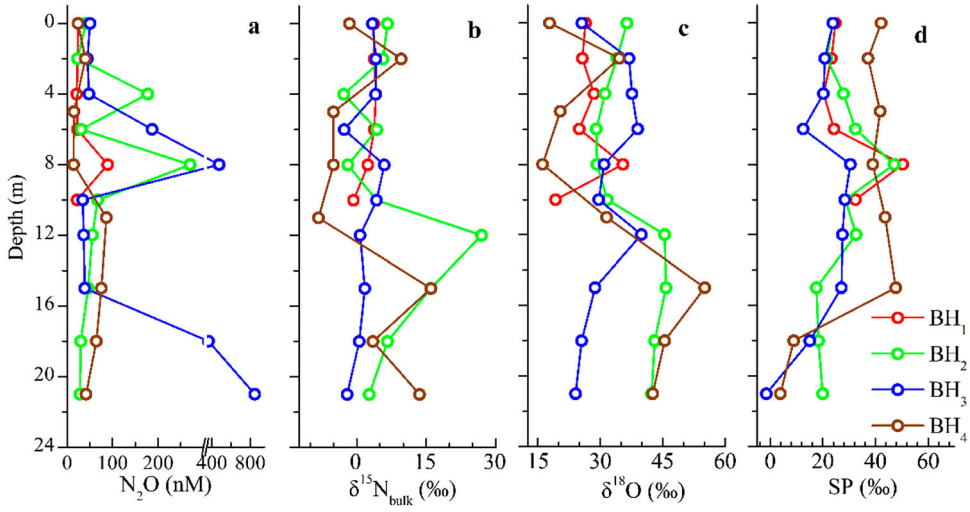

Figure 5. Water column profiles of (a) N_2O, (b) $\delta^{15}N_{bulk}$-N_2O, (c) $\delta^{18}O$-N_2O, and (d) SP–N_2O in Lake Baihua during August 2013.

and microbial respiration, can produce NH_4^+ and then NO_3^-. Significant negative relationships between DON and NO_3^- at all sites except BH_2 were indicative of the contribution of NO_3^- from degradation of organic N (Fig. 4a). The isotopic fractionation in these paths is likely to cause the nitrified NO_3^- to have a lower isotopic signature than that of the primary sources. The terrestrial inputs and high DON concentration in drainage water from the bottom of the lake might result in higher NO_3^- concentrations at BH_1 than at the other 3 sites.

At the 3 other sites, NO_3^- isotopes decreased from 12 m to the bottom of the lake subsequent with increased DON concentration. The high concentrations of DON at greater depths might be the result of phytoplankton sinking out of surface waters (Mostofa et al. 2016). Low $\delta^{18}O$-NO_3^- values might be caused by the oxygen exchange between water and NO_2^- during nitrification or by the different isotopic value of water oxygen and atmospheric oxygen used during nitrification (Casciotti et al. 2010). N characteristics in deeper water layers (>12 m) suggested that NO_3^- at those depths was primarily derived from nitrification. Furthermore, dissimilation and denitrification processes may be also involved in the 3 depth profiles and result in higher NO_3^- isotopes. The 1:1 line between $\delta^{18}O$ of NO_3^- and $\delta^{15}N$ of NO_3^- in the 0–4 m depth samples would represent assimilation along with the regeneration of NO_3^- via nitrification (Fig. 4a; Granger et al. 2010, Mayer and Wassenaar 2012).

Although mineralization and nitrification were the major N-transformations at BH_1, the NO_3^- characteristics at the bottom of BH_1 also indicated incomplete denitrification. The decrease in NO_3^- concentration from 12 m to the bottom of the lake suggested dissimilation or denitrification processes. As one of the 2 reductive N reduction pathways, however, dissimilation mostly occurred in the epilimnion. More specifically, this decrease in NO_3^- concentrations with depth was caused by denitrification. The mixing between denitrification and nitrification was the major reason for the vertical variation in the NO_3^- concentration from 12 m to the bottom of the lake, subsequently with relatively low NO_3^- concentration and isotopes and high DON.

N_2O cycling along with its isotopic characteristics in Lake Baihua

The N_2O concentration and its isotopic composition were the net result of mixing dissolved N_2O from the upper reaches (drainage water from the bottom of HF) with simultaneous production and reduction of N_2O. N_2O reduction has been thought to be more affected by low oxygen levels than other enzyme-regulated steps involved in denitrification. Moreover, enzyme-regulated steps could result in a lag phase between reduction and production of N_2O, which could possibly lead to a short-term accumulation of N_2O (Wenk et al. 2016). High fluctuations of N_2O concentration in the oxic zone, oxic–anoxic interface, and the anoxic water at depth may be linked to enhanced denitrification rates and subsequent regulation of reduction (stimulated by increased organic matter inputs following spring algal blooms).

The SP values of N_2O varying between −1.5‰ and 47.7‰ showed a slight variation in the epilimnion and a more pronounced variation in the hypolimnion, the latter of which was larger than those for other lakes (Sasaki et al. 2011, Wenk et al. 2016). The simultaneous increases in NO_3^- and N_2O concentrations between the surface and 8 m in these 3 profiles, except for at 6 m at BH_3, indicated N_2O production by nitrification. Some features can be obviously identified for NO_3^- and N_2O. For example, high SP values were found at 4 and 8 m at BH_2 and at 8 m at BH_3 with the N_2O peak and high SP value, which was interpreted as the result of nitrification processes and notably different from at 6 m at BH_3. The N_2O concentration at BH_4 was highest at 11 m, where a minimum bulk $\delta^{15}N$-N_2O (i.e., −8.3‰) occurred, indicating that *in situ* N_2O production could occur by either bacterial nitrification or nitrifier denitrification. The SP value was 43.6‰ at the depth of N_2O production, however, similar to the N_2O production at 8 m at BH_3, suggesting an NH_2OH-derived source of N_2O rather than nitrifier denitrification. Nitrification was observed for all profiles with the highest peaks for both NO_3^- and N_2O concentrations at 8 m, suggesting a simultaneous occurrence of NO_3^- regeneration and N_2O production by nitrifying microorganisms. The amount of newly produced N_2O was expected to be controlled by the newly produced NO_3^-, if nitrification was related to the N_2O accumulation in the oxic zone.

Although the isotopic evidence implied that nitrification was responsible for the increased SP values, samples at 6 m at BH_3 with considerably increased NO_3^- isotope values and decreased SP values could indicate that NO_3^- and N_2O mainly originated from denitrification processes. Denitrification was also observed in the anoxic hypolimnion (15 to 21 m) zone with decreased SP signatures and NO_3^- concentrations, suggesting the increased contribution of denitrification to N_2O production. The highest DOC concentration observed at the bottom of BH_3 and anoxic zones was conducive to denitrification. Low values of the N_2O isotopomer (SP = −1.5‰ and $\delta^{15}N_{bulk}$ = −2.1‰) at 21 m at BH_3 indicated that denitrification was responsible for the highest N_2O concentrations at this depth.

Elucidating the oxygen isotopic characteristics of N_2O is particularly challenging because its isotopic

composition reflects both source and the tendency for intermediate compounds of N_2O production (Sutka et al. 2006, Well and Flessa 2008, Zou et al. 2014). The $\delta^{18}O$ of N_2O derived from NH_2OH decomposition might depend on the $\delta^{18}O$ of O_2 during the first reaction of nitrification if the $\delta^{18}O$ of N_2O produced by nitrification and nitrifier–denitrification depended on both the $\delta^{18}O$-O_2 and $\delta^{18}O$-H_2O, which would be proportionally affected by the amount of oxygen atom exchange between NO_2^- and H_2O. This pattern is consistent with relatively more N_2O production by nitrifier–denitrification due to a significant decrease in O_2 concentration at deeper layers; thereby, a substantial contribution to the overall $\delta^{18}O$-N_2O came from H_2O.

The contribution of nitrification, denitrification, and reduction to N_2O

Relatively stable N_2O concentrations and SP values between the surface and 4 m at BH_1, BH_2, and BH_3 implied the homogeneous distribution of N_2O. The dissolved N_2O in the upper reaches might partly come from denitrification owing to the outflow from the bottom of HF. The SP signatures at those depths suggested that N_2O between the surface and 4 m was a mixture of denitrified N_2O from the upper reaches and nitrified N_2O *in situ*. The discrepancy of SP signatures between the 2 production pathways can be used to back-calculate the relative contributions of nitrification and denitrification to the N_2O production according to the following equation:

$$\delta_{measure} = \delta_{denitrification} \times (1 - f) + \delta_{nitrification} \times f, \quad (1)$$

where $\delta_{denitrification}$, $\delta_{nitrification}$, and f are denoted as the SP value for denitrification, the SP value for nitrification, and the nitrification contribution, respectively.

To further quantify the contributions of the 2 processes, the SP signature of endmembers should be determined. In this study, the high concentration of N_2O in the deep water (21 m) at the center of the lake (BH_3) suggested that denitrification was responsible for the accumulation. The low values of N_2O isotopomers and the highest N_2O concentrations in the deep water (21 m, SP = −1.5‰) at the center of the lake (BH_3), which was within the range of pure cultures from −4.0‰ to 1.9‰ (Stuka et al. 2006), can be used as a denitrification signature because of the relatively stable stratification. The SP value of hydroxylamine oxidation or nitrification from pure cultures ranged from 30.6‰ to 37.5‰, and the SP value of 33‰ was characteristic of nitrification (Stuka et al. 2006). We used an SP of −1.5‰ and 33‰ as the characteristic value of denitrification and nitrification, respectively. The contribution of N_2O production by nitrification and denitrification at BH_4 was not calculated because this site location was close to the dam and the trend of N_2O isotopic composition significantly varied compared to the other 3 sites. The contribution of nitrification in the epilimnion zone between the surface and 4 m (SP 20.2−27.8‰) was calculated to be between 70% (6.8%), 75% (9.3%), and 67% (5.8%) at BH_1, BH_2, and BH_3, respectively.

As discussed earlier, the relatively low SP value in the hypolimnion zone (15 to 21 m) can be explained by a mixture of nitrification and denitrification processes. Using the same end member information, the portion of the denitrification contribution can be calculated. The results showed that 42% (3.6%) and 57% (41%) of N_2O were produced by denitrification at BH_2 and BH_3, respectively, whereas 58% (3.6%) and 43% (41%) of N_2O were produced by nitrification at BH_2 and BH_3, respectively. Because the SP value at 21 m at BH_3 was chosen as the end member of denitrification, the denitrification contribution should be responsible for the entire N_2O production at this depth.

From 6 to 12 m, oxygen concentrations decreased with depth. This decrease may shift the N_2O production process from nitrification to denitrification and also the increase in the ratio of N_2O reduction to its production, which may induce an increase in SP value along with $\delta^{15}N_{N2O}$ and $\delta^{18}O_{N2O}$ values (Well et al. 2005, Yamagishi et al. 2007, Koba et al. 2009, Wenk et al. 2016). From the various reports of high SP values in aquatic systems, high SP values were characteristic of denitrifying aquatic environments, where N_2O reduction is favored because N_2O fluxes are restricted by low gas diffusivity (Well et al. 2005). In this study, no profiles showed a consistent increase in $\delta^{15}N$, $\delta^{18}O$, and SP values. Although higher SP values than the pure culture results were observed, N_2O reduction can be used to explore possible mechanisms for the high values. N_2O between 6 and 12 m likely resulted from mixing processes, including nitrification and denitrification, and the increase in the ratio of N_2O reduction. If the contribution of nitrification and denitrification between 6 and 12 m was the same as that between the surface and 4 m, the SP signature should have the same range as the signature between the surface and 4 m (SP 20.2–27.8‰). The proportion of N_2O reduction can be calculated using the following approximate Rayleigh linearization (Yamagishi et al. 2007, Sasaki et al. 2011):

$$\delta_{measure} = \delta_{original} + \varepsilon \times \ln(C/C_0), \quad (2)$$

where $\varepsilon = {}^{SP}\varepsilon = -16.4‰$, which is calculated from the N_2O reduction in the water column (Yamagishi et al. 2007, Sasaki et al. 2011), and $\delta_{original} = SP_{original} =$ 22.9‰, which is the average SP signature between the

surface and 4 m at BH_1, BH_2, and BH_3. C_0 and C denoted the original, not reduced, N_2O concentration and N_2O concentration after reduction, respectively. Quantitative analysis showed that the pre-existing N_2O could be reduced within the range of 24% to 77% at BH_2 and BH_3.

Although we calculated the N_2O contributions from nitrification, denitrification, and reduction based on the mixing model and Rayleigh linearization, uncertainties might still exist in those calculations. For example, unstable redox conditions between 6 and 12 m might impede the transformation of N_2O to N_2 (Wenk et al. 2016). Thus, the N_2O reduction might be overestimated between 6 and 12 m because the SP signature of nitrification can reach up to 37.5% (Frame and Casciotti 2010). The high SP signature implied that nitrification contributions between 6 and 12 m should be higher than between the surface and 4 m. Furthermore, we could not exclude the possibility of contribution of N_2O reduction between 15 and 21 m, meaning that the quantitative analysis from denitrification between 15 and 21 m might be underestimated. In addition, this calculation ignored the vertical and horizontal diffusion, which might influence the estimation based on the isotopic fractionation (Well and Flessa 2008).

Conclusion

This study investigated N biogeochemical processes and N_2O production in a typical stratified impoundment in SW China, located on a river with a large number of hydroelectric dams. The water temperature profile showed the thermocline occurred between a depth of 6 and 8 m. The DO concentration declined in the thermocline and continued to fall to <20 μM below 12 m. The DOC concentrations showed a larger variation, particularly at BH_2, whereas high concentrations of DOC were detected at the bottom of the other 3 profiles. NO_3^- concentrations and its isotopic composition varied with depth and among locations. The positive relationship between $\delta^{15}N$ and $\delta^{18}O$ of NO_3^- along with decreasing NO_3^- in the 0–4 m depth could be a signature of NO_3^- assimilation. Denitrification and nitrification were responsible for the variation of various N species from 12 m to the bottom of the lake.

High N_2O concentration and its extreme oversaturation were often detected for all depth profiles of Lake BH. Simultaneous increases in NO_3^- and N_2O concentrations at BH_1 indicated that the N_2O production could result from nitrification. The detected N_2O peaks suggested N_2O accumulation. The SP signature suggested that N_2O in the oxic zone was produced by denitrified N_2O from the upper reach and nitrified N_2O *in situ*. Low values of the N_2O isotopomers along with the highest N_2O concentrations at the bottom of this lake (SP = −1.5‰) can be used as a signature for denitrification. Although the calculation of SP gave semi-quantitative analysis for N_2O dynamic processes, we concluded that nitrification contributed >67% of the N_2O production between the surface and 4 m, which was lower than that between 6 m and 12 m. N_2O reduction is <77% between 6 and 12 m. The contribution of denitrification between 15 and 21 m was >43%. Further studies on the vertical distribution of microorganism and hydrological conditions in the key zone will help to understand N dynamics and production of greenhouse gases in hydroelectric impoundments.

Acknowledgements

This work was supported by the National Key R&D Program of China under Grant No. 2016YFA0601002; National Natural Science Foundation of China under Grant No.s 41571130072, 41403105, 41672351; and IAEA under Grant F32007. We thank Dr. Fadhlullah, Prof. Maberly, and Prof. Wang for improvement of quality. We also thank Drs. Jing Liu, Jun Zhong, Pan Li, Qiang-Sheng Huang, and Wei-Qi Lu for their help during the sample collection. We thank other members for their help for analysis assistance in Yoshida's laboratory in the Tokyo Institute of Technology, Japan. The authors declare no competing financial interests.

ORCID

Fu-Jun Yue http://orcid.org/0000-0003-3733-7216
Khan M.G. Mostofa http://orcid.org/0000-0001-5203-2432
Naohiro Yoshida http://orcid.org/0000-0003-0454-3849
Shi-Lu Wang http://orcid.org/0000-0003-0945-8686

References

Baggs EM. 2008. A review of stable isotope techniques for N_2O source partitioning in soils: recent progress, remaining challenges and future considerations. Rapid Commun Mass Sp. 22:1664–1672.

Beusen AHW, Bouwman AF, Van Beek LPH, Mogollon JM, Middelburg JJ. 2016. Global riverine N and P transport to ocean increased during the 20th century despite increased retention along the aquatic continuum. Biogeosciences. 13:2441–2451.

Casciotti KL, McIlvin M, Buchwald C. 2010. Oxygen isotopic exchange and fractionation during bacterial ammonia oxidation. Limnol Oceanogr. 55:753–762.

Finlay JC, Small GE, Sterner RW. 2013. Human influences on nitrogen removal in lakes. Science. 342:247–250.

Finlay JC, Sterner RW, Kumar S. 2007. Isotopic evidence for in-lake production of accumulating nitrate in Lake Superior. Ecol Appl. 17:2323–2332.

Frame CH, Casciotti KL. 2010. Biogeochemical controls and isotopic signatures of nitrous oxide production by a marine

ammonia-oxidizing bacterium. Biogeosciences. 7:2695–2709.
Fu PQ, Mostofa KMG, Wu FC, Liu CQ, Li W, Liao HQ, Wang LY, Wang J, Mei Y. 2010. Excitation-emission matrix characterization of dissolved organic matter sources in two eutrophic lakes (Southwestern China Plateau). Geochem J. 44:99–112.
Granger J, Sigman DM, Rohde MM, Maldonado MT, Tortell PD. 2010. N and O isotope effects during nitrate assimilation by unicellular prokaryotic and eukaryotic plankton cultures. Geochim Cosmochim Ac. 74:1030–1040.
Heil J, Wolf B, Bruggemann N, Emmenegger L, Tuzson B, Vereecken H, Mohn J. 2014. Site-specific ^{15}N isotopic signatures of abiotically produced N_2O. Geochim Cosmochim Ac. 139:72–82.
Koba K, Osaka K, Tobari Y, Toyoda S, Ohte N, Katsuyama M, Suzuki N, Itoh M, Yamagishi H, Kawasaki M, et al. 2009. Biogeochemistry of nitrous oxide in groundwater in a forested ecosystem elucidated by nitrous oxide isotopomer measurements. Geochim Cosmochim Ac. 73:3115–3133.
Liu XL. 2010. The effects of cascade reservoirs on biogeochemical cycling of nitrogen in river-reservoir system – take Wujiang River and its branch Maotiao River in SW China for example. Guiyang (China): University of Chinese Academy of Sciences.
Liu XL, Liu CQ, Li SL, Wang FS, Wang BL, Wang ZL. 2011. Spatiotemporal variations of nitrous oxide (N_2O) emissions from two reservoirs in SW China. Atmos Environ. 45:5458–5468.
Mayer B, Wassenaar LI. 2012. Isotopic characterization of nitrate sources and transformations in Lake Winnipeg and its contributing rivers, Manitoba, Canada. J Great Lakes Res. 38 (Suppl 3):135–146.
McIlvin MR, Casciotti KL. 2011. Technical updates to the bacterial method for nitrate isotopic analyses. Anal Chem. 83:1850–1856.
Mostofa KMG, Liu CQ, Vione D, Gao KS, Ogawa H. 2013. Sources, factors, mechanisms and possible solutions to pollutants in marine ecosystems. Environ Pollut. 182:461–478.
Mostofa KMG, Liu CQ, Zhai WD, Minella M, Vione D, Gao KS, Minakata D, Arakaki T, Yoshioka T, Hayakawa K, et al. 2016. Reviews and syntheses: ocean acidification and its potential impacts on marine ecosystems. Biogeosciences. 13:1767–1786.
North RL, Winter JG, Dillon PJ. 2013. Nutrient indicators of agricultural impacts in the tributaries of a large lake. Inland Waters. 3:221–234.
Ohte N, Tayasu I, Kohzu A, Yoshimizu C, Osaka K, Makabe A, Koba K, Yoshida N, Nagata T. 2010. Spatial distribution of nitrate sources of rivers in the Lake Biwa watershed, Japan: controlling factors revealed by nitrogen and oxygen isotope values. Water Resour Res. 46:W07505.
Pearson LK, Hendy CH, Hamilton DP, Silvester WB. 2012. Nitrogen-15 isotope enrichment in benthic boundary layer gases of a stratified eutrophic iron and manganese rich lake. Aquat Geochem. 18:1–19.
Santoro AE, Buchwald C, McIlvin MR, Casciotti KL. 2011. Isotopic signature of N_2O produced by marine ammonia-oxidizing archaea. Science. 333:1282–1285.
Sasaki Y, Koba K, Yamamoto M, Makabe A, Ueno Y, Nakagawa M, Toyoda S, Yoshida N, Yoh M. 2011. Biogeochemistry of nitrous oxide in Lake Kizaki, Japan, elucidated by nitrous oxide isotopomer analysis. J Geophys Res-Biogeo. 116(G4):G04030.
Spoelstra J, Schiff SL, Elgood RJ, Semkin RG, Jeffries DS. 2001. Tracing the sources of exported nitrate in the Turkey lakes watershed using $^{15}N/^{14}N$ and $^{18}O/^{16}O$ isotopic ratios. Ecosystems. 4:536–544.
Sterner RW. 2011. C:N:P stoichiometry in lake superior: freshwater sea as end member. Inland Waters. 1:29–46.
Sutka RL, Adams GC, Ostrom NE, Ostrom PH. 2008. Isotopologue fractionation during N_2O production by fungal denitrification. Rapid Commun Mass Sp. 22:3989–3996.
Sutka RL, Ostrom NE, Ostrom PH, Gandhi H, Breznak JA. 2003. Nitrogen isotopomer site preference of N_2O produced by *Nitrosomonas europaea* and *Methylococcus capsulatus* bath. Rapid Commun Mass Sp. 17:738–745.
Sutka RL, Ostrom NE, Ostrom PH, Breznak JA, Gandhi H, Pitt AJ, Li F. 2006. Distinguishing nitrous oxide production from nitrification and denitrification on the basis of isotopomer abundances. Appl Environ Microb. 72:638–644.
Toyoda S, Mutobe H, Yamagishi H, Yoshida N, Tanji Y. 2005. Fractionation of N_2O isotopomers during production by denitrifier. Soil Biol Biochem. 37:1535–1545.
Toyoda S, Yoshida N. 1999. Determination of nitrogen isotopomers of nitrous oxide on a modified isotope ratio mass spectrometer. Anal Chem. 71:4711–4718.
Toyoda S, Yoshida N. 2016. Development of automated preparation system for isotopocule analysis of N_2O in various air samples. Atmos Meas Tech. 9:2093–2101.
Wang SL, Liu CQ, Wang GJ, Tao FX, Li J, Zhu ZZ, Lv YC. 2004. Decmposition of organic matter and N_2O cycling in Lake Baihua, Guizhou, during the late stratification. Quaternary Sci. 24:569–577. Chinese with English abstract.
Well R, Flessa H, Jaradat F, Toyoda S, Yoshida N. 2005. Measurement of isotopomer signatures of N_2O in groundwater. J Geophys Res-Biogeo. 110:G02006.
Well R, Flessa H. 2008. Isotope fractionation factors of N_2O diffusion. Rapid Commun Mass Sp. 22:2621–2628.
Well R, Flessa H. 2009. Isotopologue signatures of N_2O produced by denitrification in soils. J Geophys Res-Biogeo. 114:G02020.
Wenk CB, Frame CH, Koba K, Casciotti KL, Veronesi M, Niemann H, Schubert CJ, Yoshida N, Toyoda S, Makabe A, et al. 2016. Differential N_2O dynamics in two oxygen-deficient lake basins revealed by stable isotope and isotopomer distributions. Limnol Oceanogr. 61:1735–1749.
Wenk CB, Zopfi J, Blees J, Veronesi M, Niemann H, Lehmann MF. 2014. Community N and O isotope fractionation by sulfide-dependent denitrification and anammox in a stratified lacustrine water column. Geochim Cosmochim Ac. 125:551–563.
Wu D, Koster JR, Cardenas LM, Bruggemann N, Lewicka-Szczebak D, Bol R. 2016. N_2O source partitioning in soils using ^{15}N site preference values corrected for the N_2O reduction effect. Rapid Commun Mass Sp. 30:620–626.
Xiao HY, Liu CQ. 2004. Discrimination between extraneous nitrogen input and interior nitrogen release in lakes. Sci China Ser D. 47:813–821.
Yamagishi H, Westley MB, Popp BN, Toyoda S, Yoshida N, Watanabe S, Koba K, Yamanaka Y. 2007. Role of nitrification and denitrification on the nitrous oxide cycle in the eastern tropical North Pacific and Gulf of California. J Geophys Res-Biogeo. 112:G02015.

Yoshida N, Morimoto H, Hirano M, Koike I, Matsuo S, Wada E, Saino T, Hattori A. 1989. Nitrification rates and ^{15}N abundances of N_2O and NO_3^- in the western North Pacific. Nature. 342:895–897.

Zou Y, Hirono Y, Yanai Y, Hattori S, Toyoda S, Yoshida N. 2014. Isotopomer analysis of nitrous oxide accumulated in soil cultivated with tea (*Camellia Sinensis*) in Shizuoka, central Japan. Soil Biol Biochem. 77:276–291.